의학박사 학위논문

Integrin αvβ3 induces HSP90 inhibitor resistance via FAK activation in KRAS-mutant non-small cell lung cancer

KRAS변이 양성 비소세포폐암에서 FAK활성화를 통한 Integrin αvβ3 유도 HAP90억제제 내성에 관한 연구

울산대학교 대학원

의 학 과

윤 신 교

KRAS변이 양성 비소세포폐암에서 FAK활성화를 통한 Integrin αvβ3 유도 HAP90억제제 내성에 관한 연구

지도교수 장 세 진

이 논문을 의학박사 학위 논문으로 제출함

2022년 7월

울산대학교 대학원

의 학 과

윤 신 교

윤신교의 의학박사학위 논문을 인준함

심사위원 장 세 진 (인)

심사위원 이 대 호 (인)

심사위원 김 정 은 (인)

심사위원 박 강 서 (인)

심사위원 최 윤 지 (인)

울 산 대 학 교 대 학 원

2022년 7월

Abstract

Purpose

HSP90 remains an important cancer target because of its involvement in multiple oncogenic protein pathways and biologic processes. Although many HSP90 inhibitors have been tested in the treatment of KRAS-mutant non-small cell lung cancer (NSCLC), most, including AUY922, have failed due to toxic effects and resistance generation, even though a modest efficacy has been observed for these drugs in clinical trials. In our present study, we investigated the novel mechanism of resistance to AUY922 to explore possible avenues of overcoming and want to provide some insights that may assist with the future development of successful next-generation HSP90 inhibitors.

Materials and Methods

We established two AUY922-resistant KRAS-mutated NSCLC cells and conducted RNA sequencing to identify novel resistance biomarker.

Results

We identified novel two resistance biomarkers. We observed that both integrin Av (ITGAv) and β3 (ITGB3) induce AUY922-resistance via focal adhesion kinase (FAK) activation, as well as an epithelial-mesenchymal transition (EMT), in both *in vitro* and *in vivo*

xenograft model. mRNAs of both ITGAv and ITGB3 were also found to be elevated in a patient who had shown acquired resistance in a clinical trial of AUY922. ITGAv was induced by miR-142 downregulation, and ITGB3 was increased by miR-150 downregulation during the development of AUY922-resistance. Therefore, miR-150 and miR-142 overexpression effectively inhibited ITGAvB3-dependent FAK activation, restoring sensitivity to AUY922.

Conclusion

The synergistic co-targeting of FAK and HSP90 attenuated the growth of ITGAvB3-induced AUY922-resistant KRAS-mutated NSCLC cells *in vitro* and *in vivo*, suggesting that this combination may overcome acquired AUY922-resistance in KRAS-mutant NSCLC.

Contents

Abstract 4

Introduction 8

Materials and Methods 11

Results 20

Discussion 26

References 31

Figures 36

List of figures

Figure 1. Establishment of acquired AUY922 resistance in NSCLC cells harboring a KRAS mutation..... 36

Figure 2. FAK activation via ITGAvB3 induces AUY922 resistance in KRAS-mutated NSCLC cells 38

Figure 3. Overexpression of integrin Av and integrin B3 induces AUY922 resistance in KRAS-mutated NSCLC cells..... 40

Figure 4. TSPAN7 contributes to the epithelial-mesenchymal transition of acquired AUY922-resistant cells 42

Figure 5. FAK activation via miR-150 and miR-142 downregulation induce AUY922 resistance 44

Figure 6. A FAK inhibitor, and not an integrin inhibitor, shows synergistic effects with AUY922 in AUY922-resistant cells 46

Figure 7. Schemas illustrating the identified mechanisms of acquired resistance to AUY922... 48

Supplementary Figure 1. 49

Introduction

Members of the RAS family are involved in the regulation of many signal transduction processes in normal cells. When RAS mutated, they are persistently activated and promote oncologic events, including the transcription of cancer-related genes, and cell proliferation and survival. During the last three decades however, ongoing efforts to treat RAS-mutant tumors have failed due to the inability to target the RAS oncoprotein itself. This is due to its high affinity for GTP, and its lack of a clear binding pocket due to blocking by the enzyme's farnesyltransferase and geranylgeranyl transferase. These enzymes are required RAS prenylation or the lipid posttranslational modification needed for the proper cellular localization of RAS family members, particularly KRAS and NRAS [1]. Alternatively, as mutated KRAS persistently activates its downstream signaling pathways, such as RAF/MEK(Mitogen-activated protein kinase/ERK kinase)/ERK(Extracellular-signal-regulated kinase) or PI3K(phosphatidylinositol 3-kina se)/AKT(protein kinase B)/mTOR(mammalian target of the rapamycin), agents blocking one or more downstream signaling factors could potentially be used to overcome the targeting failures. Notably in this regard, we reported previously that such a blockade was efficacious at first but subsequently became ineffective soon through activation or bypass mechanisms involving alternative pathways [2,3]. Moreover, our attempts to enhance the efficacy of this approach by blocking more targets in downstream signaling pathways

induced severe or unacceptable toxicity levels as members of the RAS family have many important functional roles in normal cells.

Fortunately, however, some recent creative approaches have revealed new binding pockets on the surface of the KRAS protein, thereby presenting potential new targeting options. Among these new possibilities, the covalent targeting of mutant KRAS, blockade of KRAS interactions with associated proteins indispensable for membrane associations, and inhibition of KRAS-driven malignant phenotypes and KRAS synthetic lethal interactions, have shown some promise as effective therapeutic pathways for KRAS-mutant tumors [4,5]. Sotorasib (AMG-510), the first new agent of this type that targets the KRAS G12C mutation, has shown clinical efficacy in solid tumors. In the NSCLC subgroup of cancers, the response rate and median progression-free survival was 32.2% and 6.3 months, respectively, to this drug while the outcomes with colorectal cancer patients were 7.1% and 4.0 months, respectively. [6]. Adagrasib (MRTX849), another agent that targets KRAS G12C, has also initially shown promising clinical activity with a response rate of 45% against NSCLC, and of 17% against colorectal cancer [7,8]. The target of these agents is limited to tumors harboring the KRAS G12C mutation however and their clinical efficacy still seems modest when compared with EGFR or ALK tyrosine kinase inhibitors. This indicates that we need new therapeutic approaches covering different types of KRAS mutations to achieve a higher clinical efficacy of

targeting agents.

Heat shock protein-90 (HSP90) has remained a viable anti-cancer target as it acts as a molecular chaperone that stabilize numerous oncogenic proteins, such as EGFR, ALK, BRAF, HER2, AKT, and MEK, that play major roles in tumor proliferation and survival. In addition, a relationship between HSP90 expression and the prognosis in cancer patients has been reported [9]. Geldanamycin [10] and radicicol [11], first-generation HSP90 inhibitors exert their anti-cancer effectiveness by pharmacologically destabilizing multiple KRAS signaling molecules [12] and subsequently, second- and third-generation HSP90 inhibitors have developed. However, despite their promise in preclinical studies, HSP90 inhibitors have displayed limited or disappointing clinical activity. In many clinical studies, these drugs achieved stable disease at best or short-lasting efficacy due to the onset of resistance. A variety of chemically potent and selective HSP90 inhibitors has been developed to date and advanced to various stages of a clinical trial [13]. Among these agents, a third generation HSP90 inhibitor targeting KRAS mutated NSCLC tumors, AUY922, was developed via a collaboration between the Institute of Cancer Research and Vernalis and was licensed to Novartis. It was withdrawn in 2012 however by Novartis after failing to show efficacy in a clinical trial as a single agent [14]. HSP90 inhibitors are still at various stages of preclinical and clinical development however as counterparts for combination therapies [9,15]. A combinational

approach might be required to overcome the limitation of HSP90 inhibitors and resistance mechanisms would need to be well characterized to find the best partners. An understanding of the underlying mechanism will also be very helpful for developing new HSP90 inhibitors [13].

MicroRNAs (miRNAs) are well known as small non-coding RNAs that regulate gene expression. A lot of studies have shown that miRNA expression is overexpressed or deregulated in most cancer [16]. In addition, there are numerous research articles regarding the functions of miRNAs in the development of drug resistance [17]. Therefore, miRNA-based anticancer therapies are being developed either alone or in combination with current targeted therapies as anti-cancer sensitizer.

In our present study, we investigated the mechanism of resistance to AUY922, to explore possible avenues of overcoming and expanding the field of HSP90 inhibitors as targeted cancer drugs and we tried to identify novel resistance biomarkers, including proteins and miRNAs, of HSP90 inhibitor and also provide some insights that may assist with the future development of successful next-generation HSP90 inhibitors.

Materials and Methods

1. Cell culture and reagents

The human KRAS-mutated NSCLC cell lines, H23, H358, H647, H1944, and A549, were purchased from the American Type Culture Collection (Manassas, VA) and grown at 37°C in 5% CO_2 using RPMI-1640 (Welgene Inc., Gyeonsan, Korea) containing 10% fetal bovine serum (FBS) and 1x penicillin-streptomycin solutions from WELGENE Inc. (KOREA). AUY922 (HSP90 inhibitor, luminespib), cilengitide trifluoroacetate (inhibitor of the αvβ3 receptor) and TAE226 (FAK inhibitor) were purchased from Selleck Chemicals (Houston, TX). These agents were each dissolved in DMSO to a final concentration of 10 mM and stored at -20°C.

2. Cell viability assay

Cell viability was measured using the CellTiter-Glo® Luminescent Cell Viability Assay (Promega, Madison, WI) in accordance with the instruction manual. Briefly, 3×10^3 cells were plated in triplicate wells in 96 microtiter plates in a volume of 90 μL. On the following day, the cells were incubated with the desired concentrations of AUY922 and/or TAE226 and/or cilengitide to a final volume of 100 μL. After 72 h, 100 μL of CellTiter-Glo reagent was added and the cells were then incubated for 10 min at room temperature. The luminescence levels were measured using a Wallac 1420 (PerkinElmer, Boston, MA).

3. Establishment of AUY922-resistant cells

To establish resistant cells, AUY922 treated to A549 and H1944 cells by continuous exposure to increasing concentrations of AUY922 (2, 5, 10, 20, 40, 80, 160, 320, 500, 750, 1000 nM). Up to 160 nM, incubate cell for 4 day in each dose and up to 1000 nM, incubate cell for 6-7 day in each dose.

4. Gene expression profiling by RNA seq

To discover differentially expressed genes, we compared mRNA expression profiles between both two AUY922 resisstant cell lines. RNA samples were purified using the RNeasy kit (Qiagen). Biotinylated cRNA was prepared using the Illumina RNA Amplification Kit (Ambion, Inc.) according to the manufacturer's directions starting with approximately 500 ng total RNA. Hybridization to the Sentrix HumanRef-8 Expression BeadChip (Illumina, Inc.), washing and scanning were performed according to the Illumina BeadStation 5006 manual (revision C). Array data processing and analysis was performed using Affymetrix Expression console1.4, R program (3.1.3), DAVID 6.7. Expression changes for individual genes were considered significant if they met 4 criteria: z-ratio above 1.4 (or below -1.4 for down-regulated genes); false detection rate <0.30; p-value of the pairwise t-test <0.05; and mean background-corrected signal intensity z-score in each comparison group is not negative. This approach provides a good balance between sensitivity and specificity in the identification of differentially expressed genes, avoiding

excessive representation of false positive and false negative regulation.

5. Establishment of an integrin αvβ3 stable cell line and miR-150/miR-142 overexpressing stable cell line

The full-length cDNA for the integrin β3 subunit was purchased from Thermo Fisher Scientific and cloned into the pLVX-IRES-Puro vector (Clontech, Mountain, CA) using XbaI and XhoI restriction sites. For integrin β3 overexpression, the cDNA of integrin β3 was cloned into the pcDNA3.0 vector. The integrin αv gene was first PCR amplified from cDNA and then subcloned into the hemagglutinin pcDNA3.0 plasmid to obtain the integrin αv expression vector. This PCR was performed using the following primers: sense, 5′-CGG GAT CCA ATG GCT GCT CCC GGG-3′, and antisense, 5′-ATT TGC GGC CGC TTA GGT TTC AGA GTT TCC TTC G-3′, and the following cycling conditions: 94°C for 3 min followed by 35 cycles of 94°C for 30 sec and 48°C for 3 min, followed by 72°C for 10 min. RNA was extracted using a RNeasy Mini Kit (#74104; Qiagen, Hilden, Germany) in accordance with the manufacturer's instructions. The RNA was then reverse transcribed via a High-Capacity cDNA Reverse Transcription Kit (#4368814, ThermoFisher, Waltham, MA). cDNAs were obtained using a QIAquick Gel Extraction Kit (#28704; Qiagen). To establish stable cell lines, the pcDNA3.0/Integrin αv and pcDNA3.0/Integrin β3 or -miR-150-5p (HmiR0306-MR04; GeneCopoeia, Rockville,

MD) and -miR-142-5p (HmiR0282-MR04; GeneCopoeia, Rockville, MD) expression vectors were transfected using lipofectamine 2000 plus (Invitrogen, Carlsbad, CA), following the manufacturer's instructions. All vectors were linearized using the AhdI (New England Biolabs, Ipswich, MA) enzyme to increase the efficiency of plasmid integration. Cells (at 70-80% confluence) were washed with Opti-MEM (Invitrogen, Carlsbad, CA), and incubated with a DNA-lipofectamine mixture (2 μg DNA and 3.5 μl lipofectamine reagent). For stable transfection, the transfected cells were selected with 500 μg/ml of the antibiotic G418 (Welgene) or 1 μg/ml of the puromycin (Welgene). Parental cells transfected with empty vectors were used as controls. Integrin αvβ3 overexpression was detected by western blotting using an anti-human integrin β monoclonal antibody (#13166; Cell Signaling Technology, Danvers, MA) and integrin αv (D2N5H) monoclonal antibody (#60896; Cell Signaling Technology). miR-150 (A25576, hsa-miR-150-5p, 477918_mir, ThermoFisher Scientific) and. miR-142 (002248, hsa-miR-142-5p, 4427975_mir, ThermoFisher Scientific). expression were measured by RT-PCR.

6. Quantitative RT-PCR.

Quantitative RT-PCR was performed using RNA isolated from NSCLC cells. Briefly, total RNA was extracted using an miRNeasy Mini Kit (217004; Qiagen), in accordance

with the manufacturer's instructions. cDNA was synthesized with a Taqman microRNA Reverse Transcription Kit (Applied Biosystems, Waltham, MA). RT-PCR was performed on a LightCycler using SYBR Green (Roche, Basel, Switzerland) and a 7900HT Fast Real-Time PCR system (Applied Biosystems). Taqman gene expression assays (miR-150: hsa-miR-150-5p, A25576, miR-142: has-miR-142-5p, 4427975, ITGB3: Hs01001469_m1, 4453320, ITGAv: Hs00233808_m1, 4331182, GAPDH: Hs03929097_g1, 4453320) were purchased from ThermoFisher Scientific. The comparative Ct method 2-ΔΔCt was used to calculate the changes in miRNA expression of all samples relative to a non-diseased sample, which was designated as the calibrator.

7. Western blot analysis

For western blotting, cell lysates were first prepared using RIPA buffer (Sigma Aldrich, St. Louis, MO) in accordance with the manufacturer's instructions. Protein samples were then applied to the wells of NuPAGE 4-20% Tris-Gly gel, electrophoresed in SDS running buffer (Invitrogen), and transferred to nitrocellulose membranes using the iBlot transfer apparatus (Invitrogen). Membranes were blocked in Tris-buffered saline containing 0.5% Tween 20 (TBS-T) and 5% BSA for 1 h at room temperature, followed by incubation with the primary antibody overnight at 4°C. On the following day, after the membranes were washed three times for 10 min each in TBS-T, HRP-conjugated

secondary antibody (Bio-Rad, Hercules, CA) in TBS-T containing 2% BSA was applied for 1 hr at room temperature. Proteins were visualized with ECL Plus enhanced chemiluminescence reagents (Amersham Biosciences, Piscataway, NJ) using G-box Chemi Systems (SynGene, Bengaluru, India). The commercial antibodies used in this study were ERK, phospho-ERK, MEK, phospho-MEK, AKT, phospho-AKT, c-Raf, TSPAN7, E-cadherin N-cadherin, cleaved PARP, PARP, ITGB3, ITGAv, HSP90, Phospho-p90RSK, RSK, Phospho-FAK and □-actin (all purchased from Cell Signaling Technology).

8. Combination index analysis

Combination effects were evaluated using a CellTiter-Glo luminescent assay in cells treated with 1,000 nM AUY922 plus increasing concentrations of TAE226 (10, 100, 200, 500, and 1000 nM) or cilengitide (10, 100, 200, 500, 1000, 2000, 5000, and 10000 nM). The fraction affected (Fa) and combination indexes (CI) were processed using CalcuSyn software (Biosoft). A CI of less than 1.0, equal to 1.0, or more than 1.0 were taken to indicate synergistic, additive, and antagonistic effects, respectively.

9. siRNA-mediated knockdowns

Human TSPAN7 proteins were knocked down in A549R cells using a final 15 nM

concentration of two TSPAN7 siRNAs (Cat#4392420, s14203, s14204) sourced from ThermoFisher Scientific. In parallel, a pool of Silencer® Select Negative Control siRNA (also at a final 15 nM concentration) was used as negative control (4390843; ThermoFisher Scientific). For all siRNA transfection experiments, we used Lipofectamine RNAiMAX reagent (Invitrogen) in accordance with the manufacturer's protocol.

10. Xenograft study

Six-week-old Balb/c-nu/nu female mice were purchased from Central Lab Animal Inc. (Seoul, Korea). An A549/ITGAvB3 xenograft model was established upon subcutaneous injection of 1×10^7 cells into the right flanks of these twelve animals. Ten days after inoculation, the mice were randomized into groups of four. NVP-AUY922 (10 mg/kg) was administered 3 days/week and TAE226 (25 mg/kg) was administered 5 days/week up to 21 days. Tumor sizes were assessed at least three times per week by caliper measurement and the lesion volumes were calculated using the following formula: tumor size (mm^3) = ($d^2 \times D$)/2, where d and D are the shortest and longest diameters of the tumor, respectively. Animal procedures were approved by the Asan Medical Centre Institutional Animal Care and Use Committee and Animal Research: Reporting In Vivo Experiments (ARRIVE) guidelines. P values and percentage of tumor growth inhibition ratio (T/C)

values were both calculated at the end of the experiment.

11. Migration and invasion assay.

CytoSelect™ 24-Well Cell Invasion and Migration assay kits were purchased from Cell Biolabs (San Diego, CA). In accordance with the manufacturer's instructions, cells were serum-starved overnight and $5x10^5$ cells in 300 µl of medium without FBS were placed in the upper chamber of a transwell plate while the lower chamber was filled with 0.5 ml of medium supplemented with 10% FBS (Welgene). To quantify the number of migratory and invading cells, crystal violet-stained cells were obtained using an extraction buffer and subjected to spectrophotometric measurements at 560 nm

Results

1. Integrin αvβ3 (ITGAv□3) induces AYU922 resistance via FAK activation

Most of the KRAS-mutant NSCLC cells tested in our current experiments were sensitive to AUY922 during the early treatment period (Figures 1A, B). We selected two KRAS mutated NSCLC cell lines, A549 and H1944, and treated them with increasing concentrations of AUY922 until they displayed resistance (Figure 1C). AUY922 was eventually unable to fully block HSP90 activity in these two AUY922-resistant cell types, which we designated A549R and H1944R (Figure 1D).

We conducted RNA sequencing analysis to identify differentially expressed genes (DEGs) between AUY922–resistant and parental sensitive cells. Among the candidate DEGs that were obtained, integrin β3 (ITGB3) was found to be the most overexpressed gene in the AUY922-resistant cells and we confirmed that this ITGB3 overexpression was associated with AUY922 resistance by western blotting (Figure 2A). In addition, we found that integrin αv (ITGAv), as a representative counterpart of integrin β3, was also overexpressed in the AUY922-resistant cells (Figure 2A). Because ITGB3 and ITGAv are well known to be regulated by miR-150 and miR-142, respectively [18-20], we confirmed that miR-150 and miR-142 were downregulated in our two AUY922 resistant NSCLC cell lines (Figure 2B). Furthermore, FAK signaling was also found to

be activated in these resistant cells, which was consistent with the well-known activation of FAK as a downstream pathway of integrin αvβ3 in various tumors (Figure 2C) [21-23].

In our present study, we further investigated whether integrin αvβ3 can induce resistance to the HSP90 inhibitor, AUY922, in KRAS-mutant NSCLC cells. We hypothesized that ITGAv□3 upregulation may induce this resistant phenotype through the activation of FAK signaling. To test this hypothesis, we first ectopically expressed integrin αv (ITGAv) and integrin β3 (ITGB3) by stable transfection in two integrin-negative parental KRAS-mutant NSCLC cells (Figure 3A). Remarkably however, ITGAvB3-transfected KRAS-mutant cells exhibited a higher IC_{50} to AUY922 than their mock-transfected counterparts (Figures 3B-D). FAK activation in these stable cells (Figure 3A) revealed that acquired AUY922 resistance might occur through FAK activation, as bypass (Figure 2C), via overexpression of both ITGAv and ITGB3. In addition, we showed that ITGAvB3-induced AUY922-resistant cells were dose-dependently killed by FAK inhibitor (TAE226, Figure 3E). We also showed decrease of pFAK expression after knockdown of ITGAv and ITGB3, respectively, as well as integrin inhibitor treatment (Figure 6E), in two AUY922 resistant cells (Figure 3F).

2. AUY922-resistant KRAS-mutated NSCLCs show an EMT tendency via TSPAN7 induction

We selected another DEG, TSPAN7 (tetraspanin 7), from the comparison of our RNA sequencing data between AUY922-resistant and -sensitive cancer cells (Figure 4A). TSPAN7-mediated EMT is well known as a key event in NSCLC migration and is regarded therefore a possible target for NSCLC therapy [24]. Although TSPAN7 has been implicated in the EMT of NSCLCs [24], the involvement of TSPAN7-mediated EMT in AUY922 resistance in KRAS-mutated NSCLCs has not been well explored. We thus examined the expression of two EMT markers (E-cadherin and N-cadherin) in our A549R and H1944R cells by western blotting analysis and observed an increased N-cadherin caused by a reduction in E-cadherin in the TSPAN7-induced resistant cells (Figure 4A). In addition, an EMT-like morphology was evident in the resistant cells (Figure 4B), as was augmented migration and invasion in Boyden chamber assays (Figure 4C). To then examine whether TSPAN7 affects AUY922 resistance, we depleted this gene in the A549R and H1944R cells using two siRNAs. This TSPAN7 depletion led to significant N-cadherin overexpression (Figure 4E). However, an CellTiter-Glo® Luminescent Cell Viability Assay indicated that the TSPAN7-depleted A549R cells were still as resistant to AUY922 as the control siRNA-expressing cells (Figure 4F).

3. The co-expression of ITGB3 and ITGAv caused by miR-150 and miR-142 downregulation induces AUY922 resistance

Previous studies have reported that TSPAN7 [24] and ITGB3 [20] are induced by microRNA-150 (miR-150) downregulation activity and that ITGAv is targeted of miR-142 [18,19,25]. Since both TSPAN7 and ITGB3 are co-direct targets of miR-150 [20,24], we examined whether this regulatory molecule controlled EMT and FAK activity through the blockade of TSPAN7 and ITGB3 expression, respectively. Indeed, miR-150 expression in our two AUY922 resistant cells, A549R and H1944R, was 4-fold lower than in their parental A549 and H1944 counterparts (Figure 2B).

Based on these results, we hypothesized that miR-150 and miR-142 may regulate FAK activation. To test this possibility, we investigated whether the restoration of miR-150 and miR-142 expression in AUY922 resistant cells (A549R and H1944R) would diminish FAK signaling. A549R and H1944R cells were transfected with miR-150 and miR-142, and its ectopic expression was confirmed by quantitative RT-PCR (qRT-PCR) (Figure 5A and 5E). As shown in Figure 5B and Figure 5F, ectopic miR-150 and miR-142 expression in A549R and H1944R cells led to a significant downregulation of phosphorylated FAK via the inhibition of ITGAvB3 formation through ITGB3 and ITGAv suppression, respectively. We next tested whether miR-150 and miR-142 could restore AUY922 sensitivity by inhibiting FAK signaling in A549R and H1944R cells. Indeed, ectopic miR-150 and miR-142 expression reversed the AUY922 resistance phenotype of these cells (Figures 5C, 5D, 5G, 5H). These results suggested that miR-150 and miR-142 could

restore AUY922 sensitivity by blocking the FAK signaling bypass via suppression of ITGB3 and ITGAv expression, respectively.

4. ITGAv□3-induced AUY922 resistance is FAK-dependent but is independent of the EMT mediated by TSPAN7.

To test whether the combined inhibition of FAK and HSP90 could be a potent strategy for overcoming ITGAv□3-mediated AUY922 resistance, we employed the Chou-Talalay method (61) using different concentrations of the integrin αvβ3 inhibitor, cilengitide, or the FAK inhibitor, TAE226, in combination with AUY922 in the AUY922-resistant cells (A549R and H1944R). TAE226 rendered A549R and H1944R cells sensitive to AUY922, with a significant degree of synergy (CI < 1) observed at all concentrations tested (Figures 6C, D). Cilengitide also rendered A549R and H1944R cells sensitive to AUY922 as part of a high-dose combination treatment (Figures 6A, B). In particular, In part of pFAK inhibition effect, the FAK inhibitor, TAE226 (100 nM), was found to be more effective than the integrin αvβ3 inhibitor, cilengitide (10 mM) in A549R cell (Figure 6E). In addition, xenograft experiments with A549/ITGAvB3 cells revealed that a TAE226 and AUY922 combination reverted the ITGAvB3-induced AUY922 resistance and significantly attenuated tumor growth in comparison with either drug alone (Figure 6F). FAK phosphorylation was less affected by AUY922 exposure in AUY922-resistant

A549/ITGAvB3 xenografts (Figure 6G), implying that the activation of FAK signaling may play a role in ITGAvB3-induced AUY922 resistance.

Discussion

During last decade, HSP90 inhibitors have been in the spotlight as treatments for other drug-resistant cancers, including KRAS-mutant tumors. At the early stage of the HSP90 inhibitor development, these agents showed potent effects against most tumor cells. However, a leading drug among this panel of inhibitors, AUY922, showed disappointing results in several clinical trials over the last three years and its development was discontinued as a single agent, even though several trials have continued to test it as part of a combination treatment regimen [9,15].

Biomarkers of first generation HSP90 inhibitors, such as ganetespib, resistance have been suggested, including MCL1 [26] and JAK [27], but resistance biomarkers for second generation HSP90 inhibitors such as AUY922 are yet to be established. Significantly, we have here identified a novel candidate target that is related to AUY922. Our RNA sequencing analysis has indicated that integrin □3 shows a 29-fold increase in acquired AUY922 resistant cells compared to the parental controls. Integrins are well known as cell adhesion molecules that connect the cytoskeleton to the extra-cellular matrix (ECM) or to other cells. These proteins consist of two noncovalently bound transmembrane α and β subunits. A blockade of integrin signaling has been demonstrated to be effective in inhibiting tumor growth, angiogenesis [28], and metastasis. Among the family members, integrin αvβ3 is highly expressed on activated endothelial cells as well

as some tumor cells, but is not expressed in resting endothelial cells or most normal organs, suggesting its potential as a target for anti-cancer therapy. Prior studies have demonstrated that integrin αvβ3 induces EGFR-TKI resistance in KRAS-mutant NSCLC, in association with fibroblast growth factor-2 (FGF2), metalloproteinase MMP-2, activated PDGF, insulin, and VEGF receptors, thereby facilitating the optimal activation of cell proliferation, invasion and preventing apoptosis [28]. In addition, integrin αvβ3 has been demonstrated to induce cancer cell proliferation and survival via the activation of focal adhesion kinase (FAK) [29].

Integrin αv is one of the few integrin α subunits that associates with multiple β units, and each resulting complex belongs to the RGD ligand group. This integrin is regulated by miR-142 and miR-31, and there is evidence that it is also regulated by miR-100. We thus confirmed that both integrin αv and integrin β3 are overexpressed in the two AUY922 resistant cell lines analyzed in our present report (Figure 2A), and established for the first time that stable integrin αvβ3 expression in cells directly induces AUY922 resistance. Interestingly, the two integrin αvβ3-overexpressing NSCLC cell lines we tested here not only showed AUY922 resistance but also indicated the involvement of FAK activation (Figure 3), a well-known downstream pathway among several integrin αvβ3 signaling mechanisms. On the other hand, TSPAN7, another identified DEG in our current analyses, was found to be increased in our two AUY922

resistant cell lines. As TSPAN7 is known to promote the migration and proliferation of lung cancer cells via an EMT [24], we observed changes in the expression of EMT-related markers in AUY922-resistant cells i.e. overexpressed N-cadherin and downregulated E-cadherin (Figure 4A). When TSPAN7 was knocked down by two different siRNAs, the E-cadherin level was restored in the AUY922-resistant cells (Figure 4E). However, this EMT change caused by TSPAN7 did not affect the AUY922 sensitivity of the cells (Figure 4F).

To elucidate how ITGAv and ITGB3 become overexpressed in AUY922-resistant cells, we explored the possible role of miRNAs which are known regulate integrins [25]. Integrin β3 is also known to be regulated by several different miRNAs. For example, miR-30 is significantly reduced when integrin β3 expression is significantly increased in breast tumor initiating cells (BT-ICs)[30]. miR-150 has also been shown to regulate megakaryocyte-erythrocyte progenitor (MEP) cell development and the expression of integrin β3 on the surface of differentiated cells [30]. Moreover, miR-150 is expressed in various cancers, including cervical cancer and NSCLC [30,31] and promotes cell proliferation, migration and invasion [32].

Our present results showed that ITGAv and ITGB3 are increased by miR-142 and miR-150, respectively (Figures 2A and 2B). As miR-150 is reportedly an upstream regulator of EMT via TSPAN7 expression and contributes to ITGAvB3 complex

formation via ITGB3 overexpression, we also showed that integrin αvβ3 overexpressing AUY922-resistant cells had downregulated miR-150 and miR-142 expression (Figure 2B). In addition, the upregulation of miR-150 and miR-142 in our AUY922-resistant cell lines restored AUY922 sensitivity, which occurred through the suppression of FAK activation (Figure 5) because ITGB3 and ITGAv could not be expressed, respectively. Accordingly, we assessed whether a combination of a FAK inhibitor (TAE226) or integrin inhibitor (cilengitide) with the AUY922 HSP90 inhibitor had a synergistic effect both *in vitro* and *in vivo*. The dual inhibition of FAK and HSP90 was a more potently synergistic combination treatment in the two AUY922 resistant cell lines and in xenograft tumors (Figures 6A-6D, 6F) and interestingly, FAK inhibition was maintained for longer by a dual blockade of FAK and HSP90 than of integrin and HSP90 (Figure 6E). This FAK and HSP90 combination inhibitor treatment induced a greater apoptotic response, which may be more important in terms of killing effect in stable ITGAvB3 expressing cells (A549/ITGAvB3; Figure 6G).

It was fortunate in our present analyses that we could check the mRNA levels of both ITGAv and ITGB3 in the tumor tissue obtained from a patient who had participated into a clinical trial of AUY922 and developed drug resistance. Although the sample was obtained from one patient only, we showed clinical correlation between ITGAvB3 expression and AUY922 resistance (Supplementary Figure 1A). Our present study

findings suggest that the overexpression of ITGAv and ITGB3 is caused by miR-142 and miR-150 suppression, respectively. The induction of integrin AvB3 (ITGAvB3) will eventually result in AUY922 resistance via FAK activation, and therefore, the combination of a FAK inhibitor (TAE226), and not and integrin inhibitor, with a HSP90 inhibitor (AUY922) may be an effective strategy for overcoming ITGAvB3-induced acquired resistance (Figure 7), or for preventing the occurrence of the resistance in KRAS mutated tumors, or at least NSCLCs. We also suggest from these findings that next-generation HSP90 inhibitors could be more effective if they target both HSP90 and FAK.

References

1. Berndt N, Hamilton AD, Sebti SM. Targeting protein prenylation for cancer therapy. Nat Rev Cancer. 2011;11:775-791.

2. Park KS, Oh B, Lee MH, Nam KY, Jin HR, Yang H, et al. The HSP90 inhibitor, NVP-AUY922, sensitizes KRAS-mutant non-small cell lung cancer with intrinsic resistance to MEK inhibitor, trametinib. Cancer Lett. 2016;372:75-81.

3. Park KS, Yang H, Choi J, Seo S, Kim D, Lee CH, et al. The HSP90 inhibitor, NVP-AUY922, attenuates intrinsic PI3K inhibitor resistance in KRAS-mutant non-small cell lung cancer. Cancer Lett. 2017;406:47-53.

4. Papke B, Der CJ. Drugging RAS: Know the enemy. Science. 2017;355:1158-1163.

5. Ostrem JM, Shokat KM. Direct small-molecule inhibitors of KRAS: from structural insights to mechanism-based design. Nat Rev Drug Discov. 2016;15:771-785.

6. Hong DS, Fakih MG, Strickler JH, Desai J, Durm GA, Shapiro GI, et al. KRAS(G12C) Inhibition with Sotorasib in Advanced Solid Tumors. N Engl J Med. 2020;383:1207-1217.

7. Janne PA, Rybkin II, Spira AI, Riely GJ, Papadopoulos KP, Sabari JK, et al. KRYSTAL-1: Activity and Safety of Adagrasib (MRTX849) in Advanced/ Metastatic Non-Small-Cell Lung Cancer (NSCLC) Harboring KRAS G12C

Mutation. Eur J Cancer. 2020;138:S1-S2.

8. Johnson ML, Ou SHI, Barve M, Rybkin II, Papadopoulos KP, Leal TA, et al. KRYSTAL-1: Activity and Safety of Adagrasib (MRTX849) in Patients with Colorectal Cancer (CRC) and Other Solid Tumors Harboring a KRAS G12C Mutation. Eur J Cancer. 2020;138:S2-S2.

9. Garcia-Carbonero R, Carnero A, Paz-Ares L. Inhibition of HSP90 molecular chaperones: moving into the clinic. Lancet Oncol. 2013;14:e358-369.

10. Whitesell L, Mimnaugh EG, De Costa B, Myers CE, Neckers LM. Inhibition of heat shock protein HSP90-pp60v-src heteroprotein complex formation by benzoquinone ansamycins: essential role for stress proteins in oncogenic transformation. Proc Natl Acad Sci U S A. 1994;91:8324-8328.

11. Schulte TW, Akinaga S, Soga S, Sullivan W, Stensgard B, Toft D, et al. Antibiotic radicicol binds to the N-terminal domain of Hsp90 and shares important biologic activities with geldanamycin. Cell Stress Chaperones. 1998;3:100-108.

12. Whitesell L, Lindquist SL. HSP90 and the chaperoning of cancer. Nat Rev Cancer. 2005;5:761-772.

13. Neckers L, Blagg B, Haystead T, Trepel JB, Whitesell L, Picard D. Methods to validate Hsp90 inhibitor specificity, to identify off-target effects, and to rethink approaches for further clinical development. Cell Stress Chaperones.

2018;23:467-482.

14. Sidera K, Patsavoudi E. HSP90 inhibitors: current development and potential in cancer therapy. Recent Pat Anticancer Drug Discov. 2014;9:1-20.

15. Seggewiss-Bernhardt R, Bargou RC, Goh YT, Stewart AK, Spencer A, Alegre A, et al. Phase 1/1B trial of the heat shock protein 90 inhibitor NVP-AUY922 as monotherapy or in combination with bortezomib in patients with relapsed or refractory multiple myeloma. Cancer. 2015;121:2185-2192.

16. Ambros V. The functions of animal microRNAs. Nature. 2004;431:350-355.

17. Ma J, Dong C, Ji C. MicroRNA and drug resistance. Cancer Gene Ther. 2010;17:523-531.

18. Schwickert A, Weghake E, Bruggemann K, Engbers A, Brinkmann BF, Kemper B, et al. microRNA miR-142-3p Inhibits Breast Cancer Cell Invasiveness by Synchronous Targeting of WASL, Integrin Alpha V, and Additional Cytoskeletal Elements. PLoS One. 2015;10:e0143993.

19. Borschel CS, Stejskalova A, Schafer SD, Kiesel L, Gotte M. miR-142-3p Reduces the Size, Migration, and Contractility of Endometrial and Endometriotic Stromal Cells by Targeting Integrin- and Rho GTPase-Related Pathways That Regulate Cytoskeletal Function. Biomedicines. 2020;8.

20. Honda N, Jinnin M, Kira-Etoh T, Makino K, Kajihara I, Makino T, et al. miR-150

down-regulation contributes to the constitutive type I collagen overexpression in scleroderma dermal fibroblasts via the induction of integrin beta3. Am J Pathol. 2013;182:206-216.

21. Guan JL. Integrin signaling through FAK in the regulation of mammary stem cells and breast cancer. IUBMB Life. 2010;62:268-276.

22. Alanko J, Ivaska J. Endosomes: Emerging Platforms for Integrin-Mediated FAK Signalling. Trends Cell Biol. 2016;26:391-398.

23. Mitra SK, Schlaepfer DD. Integrin-regulated FAK-Src signaling in normal and cancer cells. Curr Opin Cell Biol. 2006;18:516-523.

24. Wang X, Lin M, Zhao J, Zhu S, Xu M, Zhou X. TSPAN7 promotes the migration and proliferation of lung cancer cells via epithelial-to-mesenchymal transition. Onco Targets Ther. 2018;11:8815-8822.

25. Chen W, Harbeck MC, Zhang W, Jacobson JR. MicroRNA regulation of integrins. Transl Res. 2013;162:133-143.

26. Busacca S, Law EW, Powley IR, Proia DA, Sequeira M, Le Quesne J, et al. Resistance to HSP90 inhibition involving loss of MCL1 addiction. Oncogene. 2016;35:1483-1492.

27. Mumin NH, Drobnitzky N, Patel A, Lourenco LM, Cahill FF, Jiang Y, et al. Overcoming acquired resistance to HSP90 inhibition by targeting JAK-STAT

signalling in triple-negative breast cancer. BMC Cancer. 2019;19:102.

28. Kumar CC. Integrin alpha v beta 3 as a therapeutic target for blocking tumor-induced angiogenesis. Curr Drug Targets. 2003;4:123-131.

29. Guo W, Giancotti FG. Integrin signalling during tumour progression. Nat Rev Mol Cell Biol. 2004;5:816-826.

30. Lu J, Guo S, Ebert BL, Zhang H, Peng X, Bosco J, et al. MicroRNA-mediated control of cell fate in megakaryocyte-erythrocyte progenitors. Dev Cell. 2008;14:843-853.

31. Suetsugu T, Koshizuka K, Seki N, Mizuno K, Okato A, Arai T, et al. Downregulation of matrix metalloproteinase 14 by the antitumor miRNA, miR-150-5p, inhibits the aggressiveness of lung squamous cell carcinoma cells. Int J Oncol. 2018;52:913-924.

32. Zhang Z, Wang J, Li J, Wang X, Song W. MicroRNA-150 promotes cell proliferation, migration, and invasion of cervical cancer through targeting PDCD4. Biomed Pharmacother. 2018;97:511-517.

Figures

Figure 1. Establishment of acquired AUY922 resistance in NSCLC cells harboring a KRAS mutation.

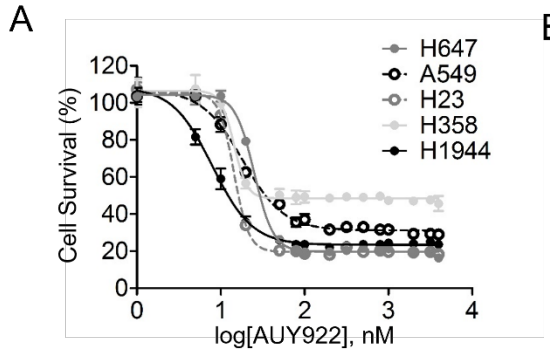

Cell lines	Histology	AUY922 IC50 (nM)
H1944	Adenocarcinoma	8
H358	Bronchioabeolar	14
H23	Adenocarcinoma	14
A549	Adenocarcinoma	18
H647	Adenosquamous	25

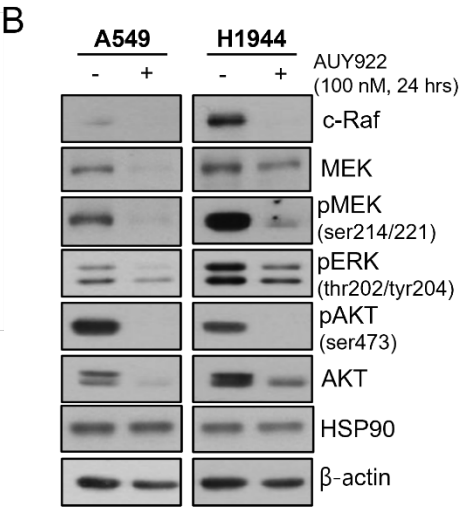

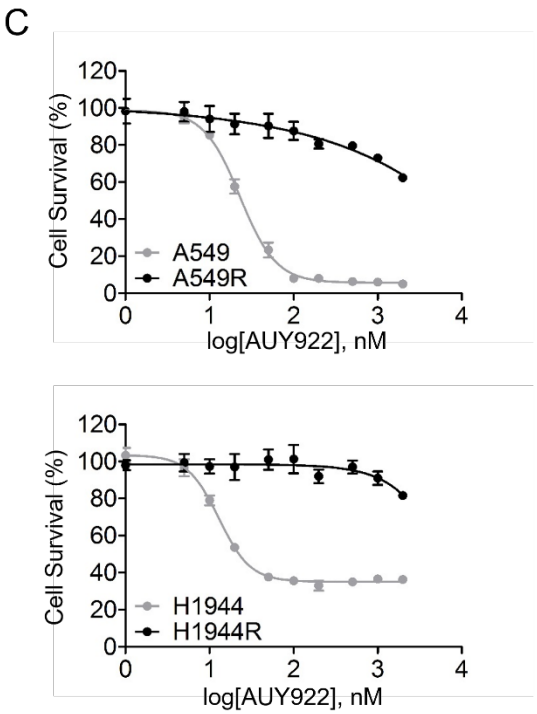

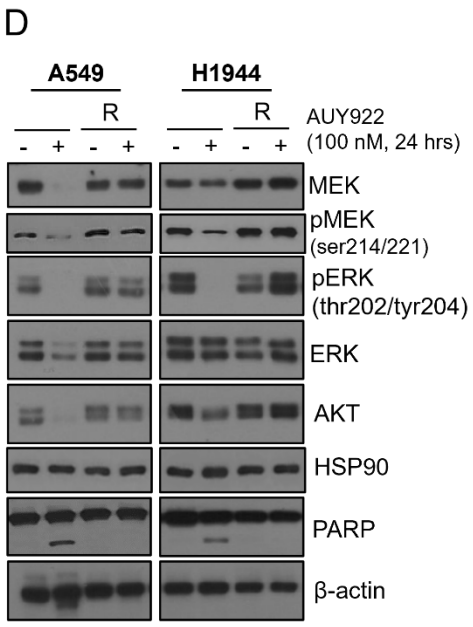

(A) Antitumor effects of AUY922 alone against three KRAS mutated NSCLC cell lines. NSCLC cells were treated with different concentrations of AUY922 for 72 h. The results are expressed as a mean ± SD of three independent experiments. (B) Results of western blotting analysis showing the endogenous protein levels in two KRAS-mutated NSCLC cell lines, A549 and H1944, after AUY922 treatment. (C) Anti-cancer effect of lapatinib in the A549 and H1944 cells, and their acquired AUY922-resistant counterparts, A549R and H1944R. Cell proliferation was measured using a CellTiter-Glo luminescent cell viability assay. The average results ± SD of three independent experiments are shown. (D) Western blotting analysis of MEK, pMEK, pERK, ERK, AKT, HSP90 and PARP expression following incubation with increasing doses of AUY922 in the A549, A549R, H1944 and H1944R cell lines. β-Actin was included as a loading control (R: Resistant cells).

Figure 2. FAK activation via ITGAvB3 induces AUY922 resistance in KRAS-mutated NSCLC cells.

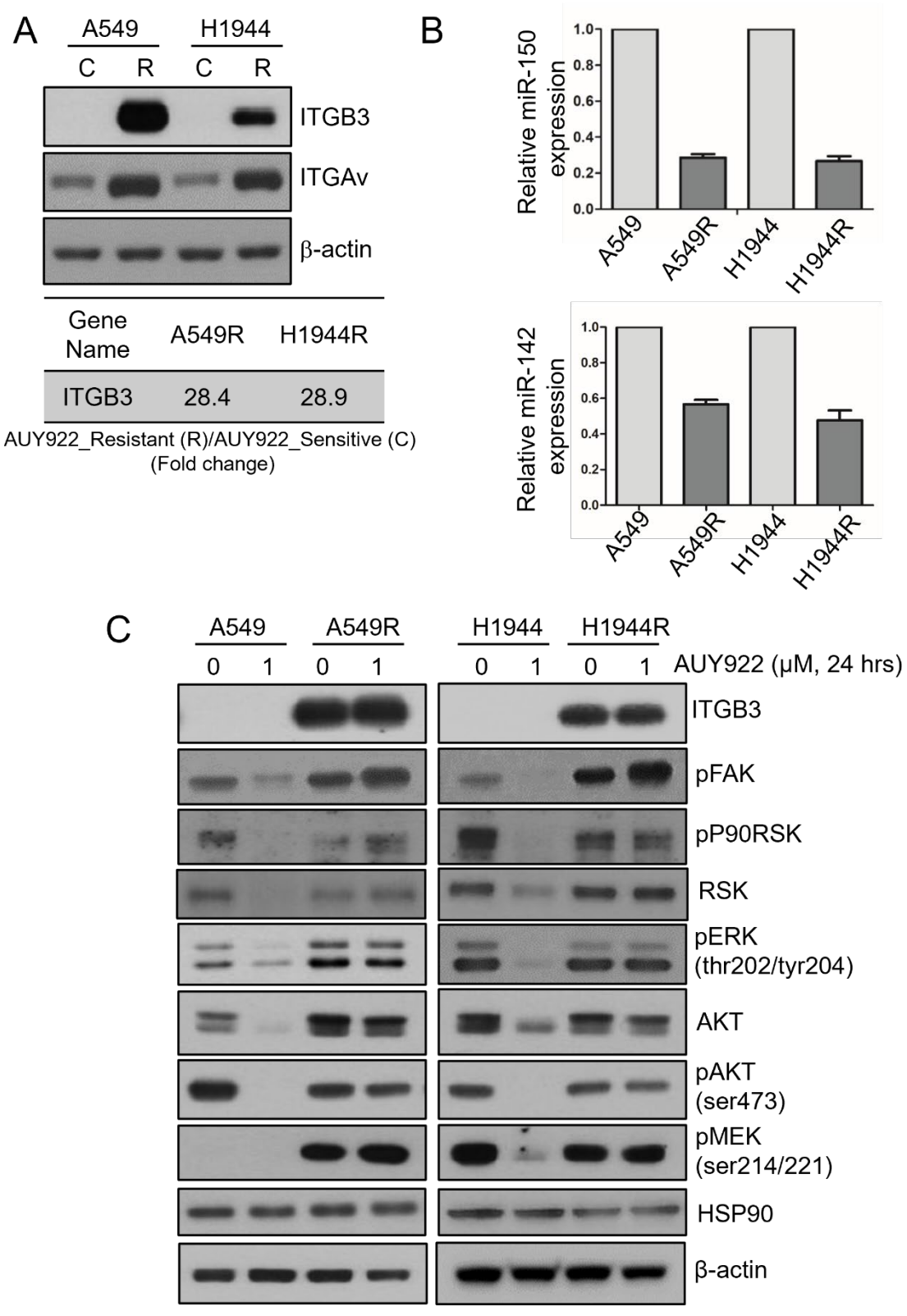

(A) Western blot analysis of the ITGB3 and ITGAv proteins in the acquired AUY922-resistant NSCLC cell lines (A549R and H1944R). (B) Real-time PCR analysis of miR-150 and miR-142 expression in the acquired AUY922-resistant NSCLC cell lines. (C) Western blotting analysis of ITGB3, pFAK, pRSK, RSK, pERK, AKT, pAKT, pMEK and HSP90 expression in A549, A549R, H1944 and H1944R cell lines following incubation with 1 □M of AUY922. β-Actin was included as a loading control.

Figure 3. Overexpression of integrin Av and integrin B3 induces AUY922 resistance in KRAS-mutated NSCLC cells.

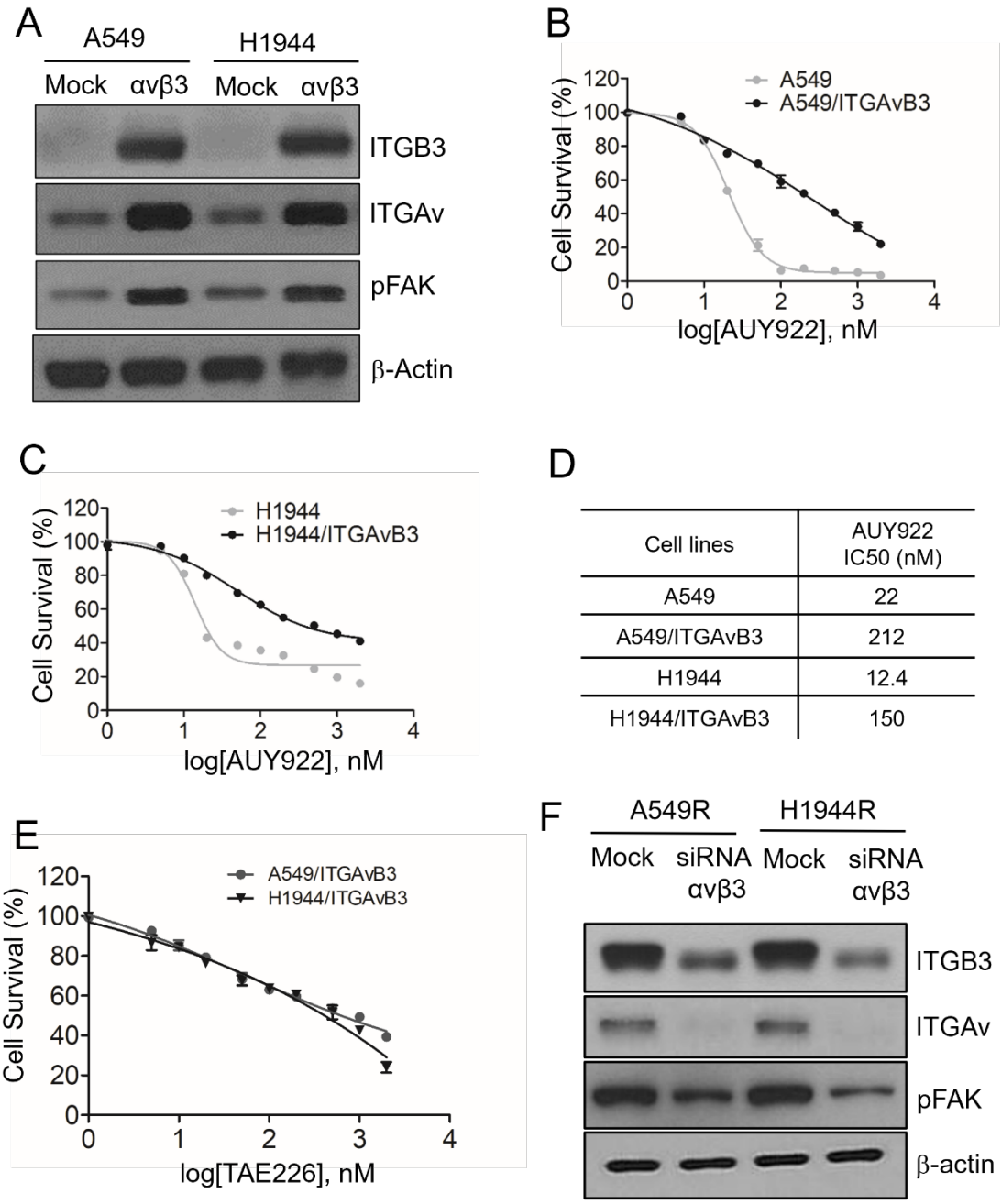

(A) Western blot analysis of ITGB3, ITGAv and pFAK proteins in stably ITGAv and ITGB3 expressing NSCLC cell lines. (B and C) Effect of ITGAv and ITGB3 on AUY922 sensitivity of two KRAS-mutant NSCLC cell lines, A549/ITGAvB3 and

H1944/ITGAvB3. CellTiter-Glo® Luminescent Cell Viability Assays were performed 72 h after drug treatment. Data represent the mean ± SD of triplicate measurements relative to untreated cells. (D) IC_{50} values are reported in the table. (E) Anti-apoptotic effect of TAE226 in A549/ITGAvB3 and H1944/ITGAvB3 cell lines. CellTiter-Glo® Luminescent Cell Viability Assays were performed 72 h after drug treatment. (F) Western blot analysis of ITGB3, ITGAv and pFAK proteins in stably ITGAv and ITGB3 knock-downed AUY922-resistant NSCLC cell lines.

Figure 4. TSPAN7 contributes to the epithelial-mesenchymal transition of acquired AUY922-resistant cells.

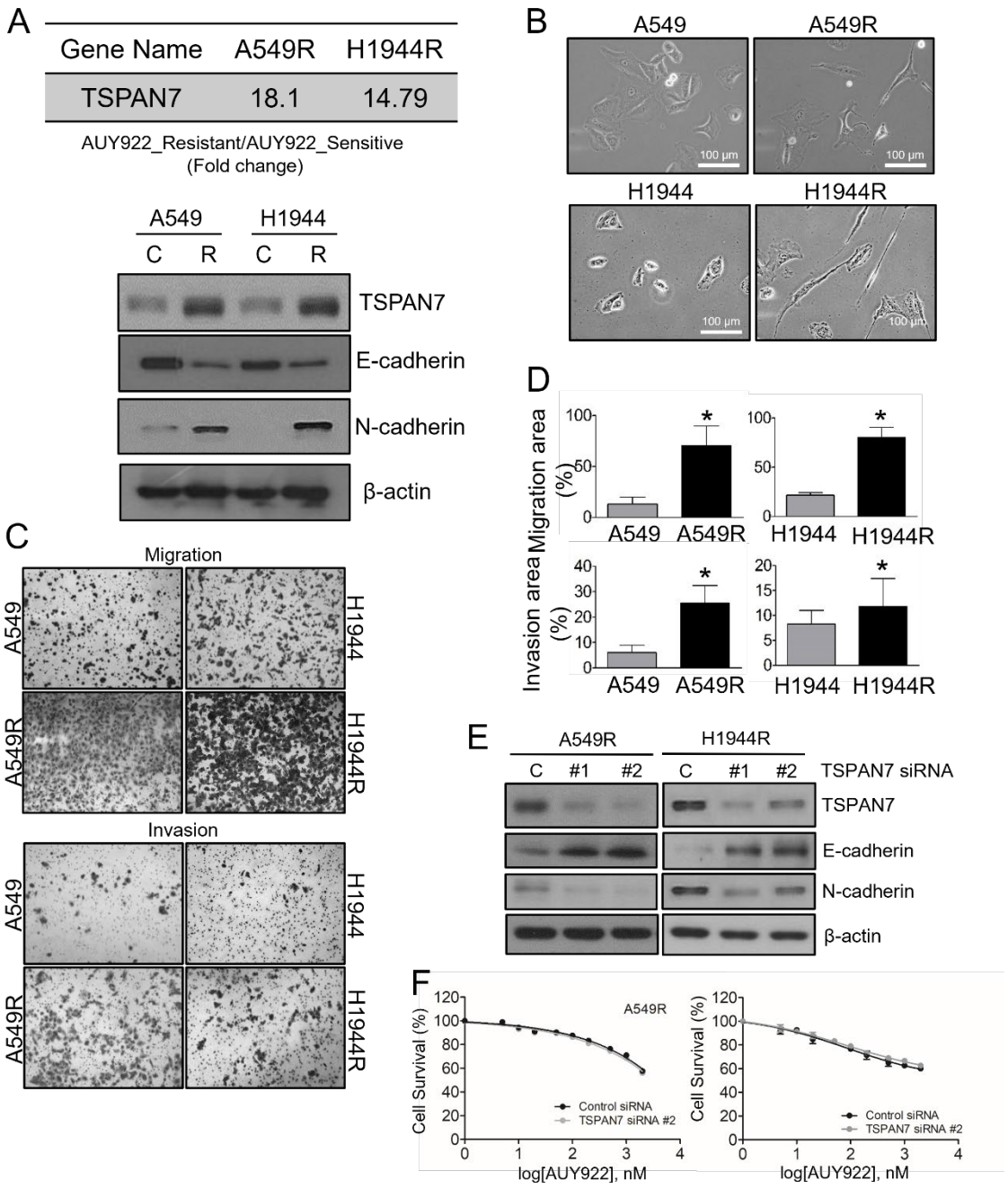

(A) Western blot analysis of the EMT signaling proteins, TSPAN7, E-Cadherin and N-Cadherin, in the two AUY922 resistant NSCLC cell lines, A549R and H1944R. (B)

Phase-contrast images of the A549R and H1944R cells revealing notable morphological changes; original magnification, x 200. (C and D) Migration and invasion assay of the A549R and H1944R cells. These NSCLC cell lines were serum starved for 24 h and cell migration and invasion assays were conducted at 48 h. Cell migration and invasion indexes were measured as described in the Methods. Data are representative of three independent experiments. (E) Western blot analysis of A549R and H1944R cells at 72 h after TSPAN7 siRNA transfection. □-actin was used as a loading control. (F) TSPAN7 siRNA could not rescue the AUY922 sensitivity in A549R and H1944R cells. Two days after transfection, two cell lines were treated with AUY922 for three days, followed by cell viability assay. The data represent triplicate experiments.

Figure 5. FAK activation via miR-150 and miR-142 downregulation induce AUY922 resistance.

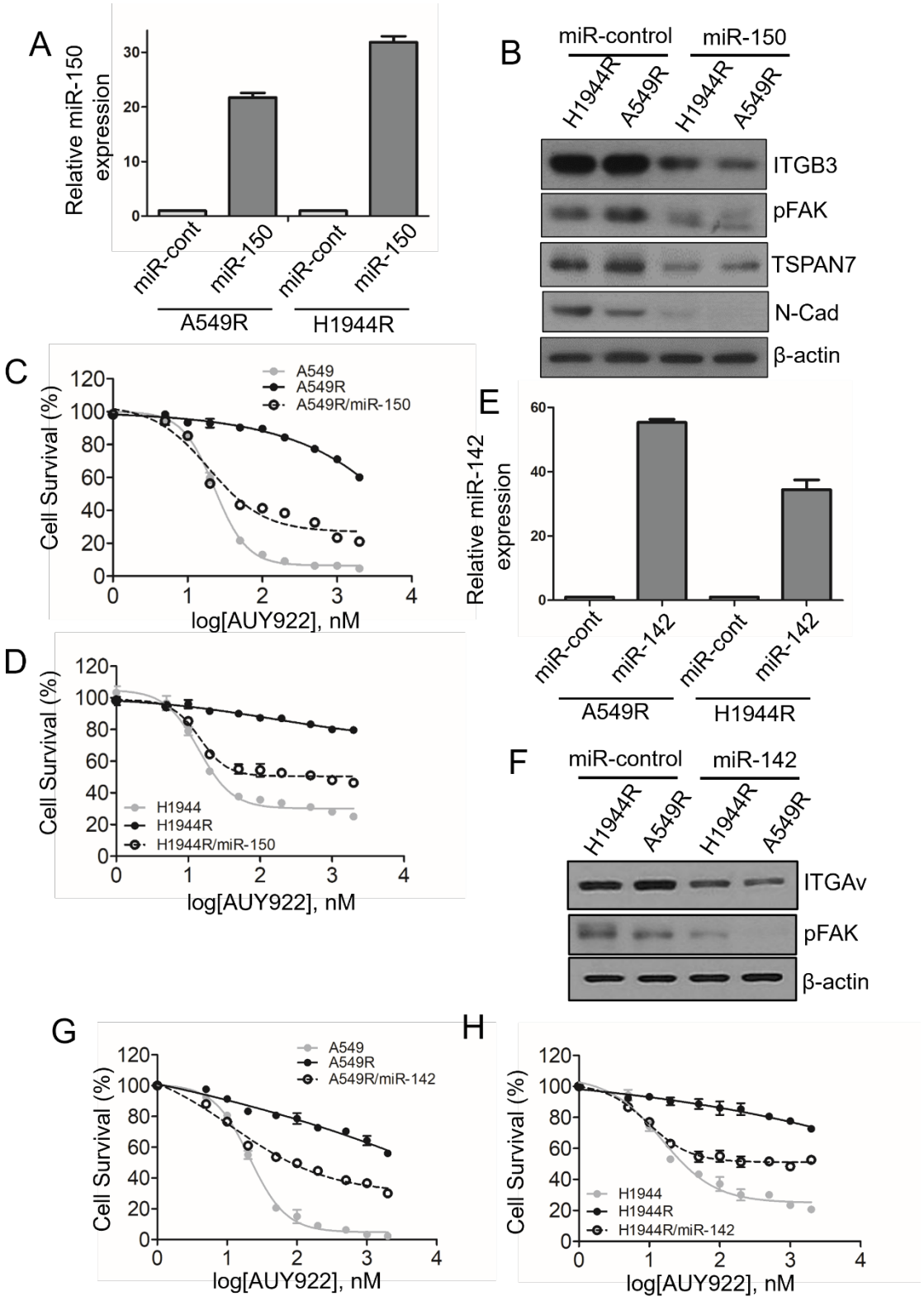

(A) Real-time PCR analysis of ectopic miR-150 expression in A549R/miR-150 and H1944/miR-150 stable cells. (B) Effect of ectopic miR-150 expression on ITGB3, pFAK, TSPAN7 and N-cadherin in miR-control and miR-150 transfected resistant cells, revealed by western blot analysis. (C and D) Ectopic miR-150 expression renders A549R and H1944R cells sensitive to AUY922. Cell viability assays were performed at 72 h after AUY922 treatment of the indicated cells at different concentrations. Data represent the mean ± SD of triplicate experiments relative to untreated cells. (E) Real-time PCR analysis of ectopic miR-142 expression in A549R/miR-142 and H1944/miR-142 stable cells. (F) Effect of ectopic miR-142 expression on ITGB3, pFAK in miR-control and miR-142 transfected resistant cells, revealed by western blot analysis. (G and H) Ectopic miR-142 expression renders A549R and H1944R cells sensitive to AUY922. Cell viability assays were performed at 72 h after AUY922 treatment of the indicated cells at different concentrations. Data represent the mean ± SD of triplicate experiments relative to untreated cells.

Figure 6. A FAK inhibitor, and not an integrin inhibitor, shows synergistic effects with AUY922 in AUY922-resistant cells.

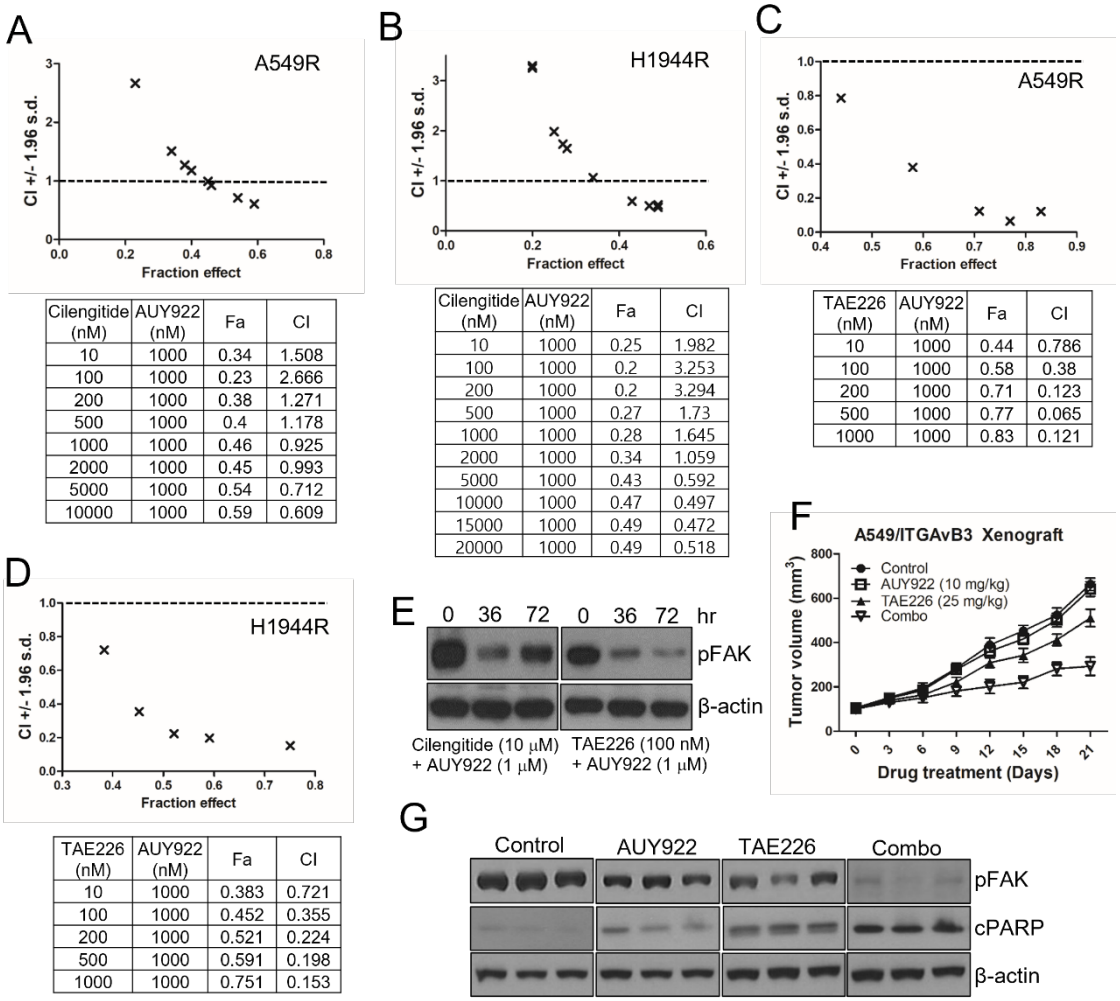

Cilengitide (nM)	AUY922 (nM)	Fa	CI
10	1000	0.34	1.508
100	1000	0.23	2.666
200	1000	0.38	1.271
500	1000	0.4	1.178
1000	1000	0.46	0.925
2000	1000	0.45	0.993
5000	1000	0.54	0.712
10000	1000	0.59	0.609

Cilengitide (nM)	AUY922 (nM)	Fa	CI
10	1000	0.25	1.982
100	1000	0.2	3.253
200	1000	0.2	3.294
500	1000	0.27	1.73
1000	1000	0.28	1.645
2000	1000	0.34	1.059
5000	1000	0.43	0.592
10000	1000	0.47	0.497
15000	1000	0.49	0.472
20000	1000	0.49	0.518

TAE226 (nM)	AUY922 (nM)	Fa	CI
10	1000	0.44	0.786
100	1000	0.58	0.38
200	1000	0.71	0.123
500	1000	0.77	0.065
1000	1000	0.83	0.121

TAE226 (nM)	AUY922 (nM)	Fa	CI
10	1000	0.383	0.721
100	1000	0.452	0.355
200	1000	0.521	0.224
500	1000	0.591	0.198
1000	1000	0.751	0.153

(A and B) Synergistic effect of a cilengitide and AUY922 combination. Cell viability assays were performed in A549R and H1944R cells treated with 1000 nM of AUY922 plus increasing concentrations of cilengitide for three days. (C and D) Synergistic effect of a TAE226 and AUY922 combination. Cell viability assays were performed in A549R and H1944R cells treated with 1000 nM of AUY922 plus increasing concentrations of TAE226 for three days. The confidence interval (CI) was calculated using CalcuSyn

software. (E) Western blot analysis of pFAK in A549R cells after each combination treatment. (F) Twelve mice harboring subcutaneous xenograft tumors derived from A549/ITGAvB3 cells were randomized into four groups. After the tumor volume reached 100 mm^3, AUY922 at 10 mg/kg was administered 3 days/week, and TAE226 (25 mg/kg) was administered 5 days/week for up to 21 days. The tumor size was assessed at least three times a week. (G) Western blotting analysis detected cleaved PARP in the mouse xenograft tumors.

Figure 7. Schemas illustrating the identified mechanisms of acquired resistance to AUY922

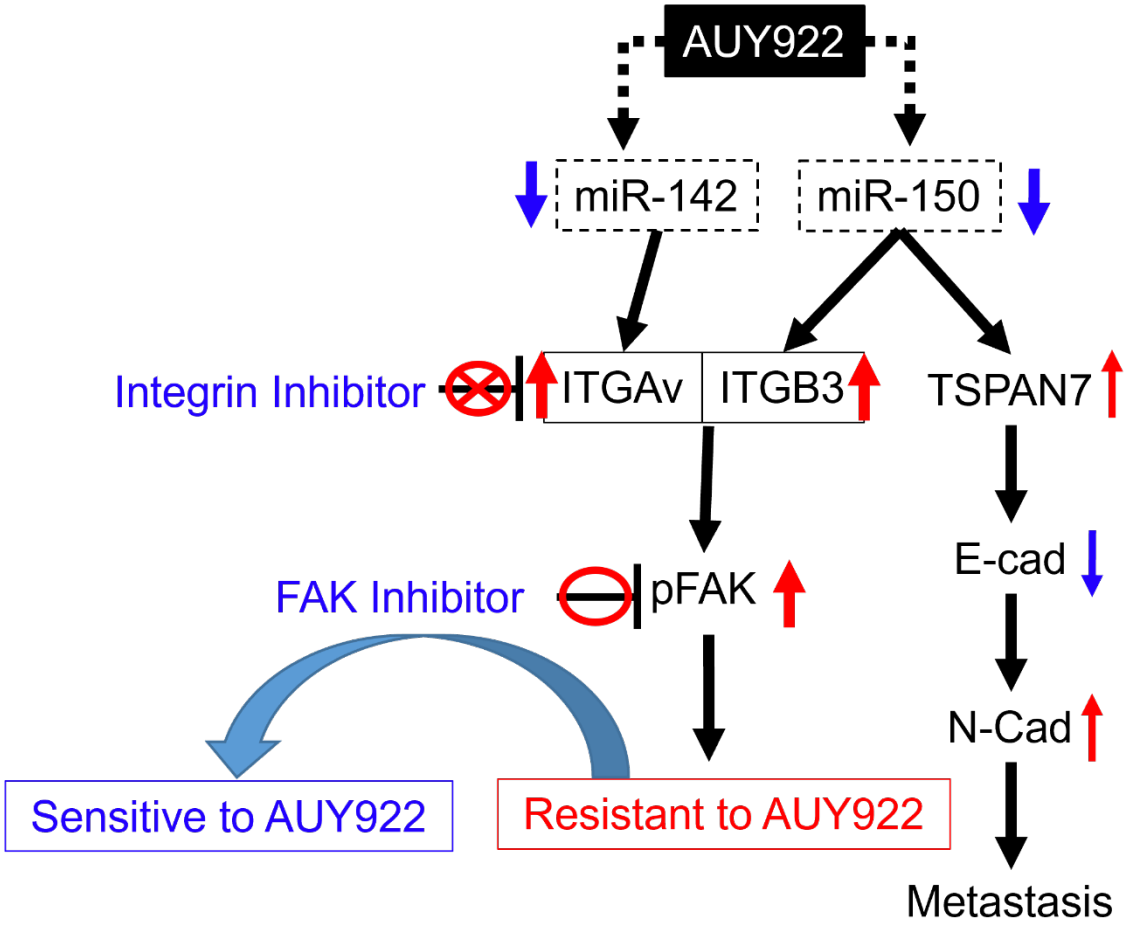

Supplementary Figure 1.

Increase of ITGAv and ITGB3 mRNA in an acquired AUY922-resistant FFPE sample cells from a patient, determined by real-time PCR analysis.